JOC Article
pubs.acs.org/joc

Isotruxene-Derived Cone-Shaped Organic Dyes for Dye-Sensitized Solar Cells

Shih-Hsun Lin,[†] Ying-Chan Hsu,[‡] Jiann T. Lin,*[,‡] Cheng-Kai Lin,[†] and Jye-Shane Yang*[,†]

[†]*Department of Chemistry, National Taiwan University, Taipei, 10617 Taiwan, and* [‡]*Institute of Chemistry, Academia Sinica, Taipei, 11529, Taiwan*

jsyang@ntu.edu.tw; jtlin@chem.sinica.edu.tw

Received September 16, 2010

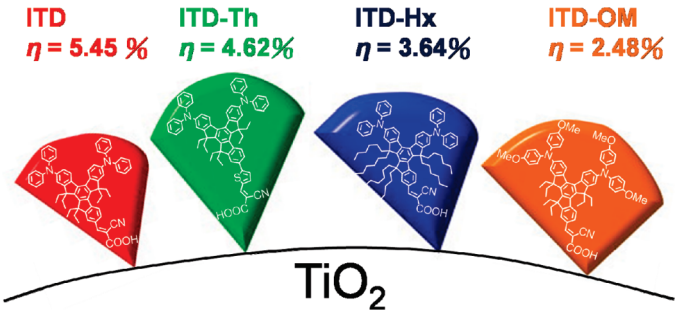

The synthesis, electronic properties, and performance in dye-sensitized solar cells (DSSCs) of four cone-shaped organic dyes (**ITD**, **ITD-Th**, **ITD-Hx**, and **ITD-OM**) containing the isotruxene π-scaffold are reported. Selective substitution of the unsymmetrical isotruxene core with two diarylamino donors and one cyanocarboxylic acid acceptor was achieved by using a prefunctionalized dibromoisotruxene building block. The ortho-para-branched isotruxene core allows strong electronic couplings among the donors and the acceptor, leading to red-shifted absorption profiles with significant charge-transfer character. All four isotruxene dyes display reversible anodic waves in cyclic voltammagrams with both HOMO and LUMO potentials suitable for application in DSSCs. The DSSCs fabricated with these cone-shaped organic dyes exhibited high open-circuit voltages (0.67−0.76 V) and fill factors (0.67−0.72) with a power conversion efficiency (η) up to 5.45%, which is 80% of the ruthenium dye N719-based standard cell fabricated and measured under the same conditions.

Introduction

Dye-sensitized solar cells (DSSCs) have emerged as one of the most attractive photovoltaic devices. To date, a variety of transition-metal complexes[1−4] and metal-free organic sensitizers[5−10] have been explored in order to improve the performance of DSSCs and to understand the structure−property relationship. Because of the advantages of low cost, easy

(1) (a) O'Regan, B.; Grätzel, M. *Nature* **1991**, *353*, 737–740. (b) Robertson, N. *Angew. Chem., Int. Ed.* **2006**, *45*, 2338–2345. (c) Ardo, S.; Meyer, G. J. *Chem. Soc. Rev.* **2009**, *38*, 115–164. (d) Imahori, H.; Umeyama, T.; Ito, S. *Acc. Chem. Res.* **2009**, *42*, 1809–1818.

(2) (a) Gao, F.; Wang, Y.; Shi, D.; Zhang, J.; Wang, M.; Jing, X.; Humphry-Baker, R.; Wang, P.; Zakeeruddin, S. M.; Grätzel, M. *J. Am. Chem. Soc.* **2008**, *130*, 10720–10728. (b) Cao, Y.; Bai, Y.; Yu, Q.; Cheng, Y.; Liu, S.; Shi, D.; Gao, F.; Wang, P. *J. Phys. Chem. C* **2009**, *113*, 6290–6297. (c) Bessho, T.; Zakeeruddin, S. M.; Yeh, C.-Y.; Diau, E. W.-G.; Grätzel, M. *Angew. Chem., Int. Ed.* **2010**, *49*, 6646–6649.

(3) Nazeeruddin, M. K.; Angelis, F. D.; Fantacci, S.; Selloni, A.; Viscardi, G.; Liska, P.; Ito, S.; Takeru, B.; Grätzel, M. *J. Am. Chem. Soc.* **2005**, *127*, 16835–16847.

(4) Chen, C.-Y.; Wang, M.; Li, J.-Y.; Pootrakulchote, N.; Alibabaei, L.; Ngoc-le, C.-H.; Decoppet, J.-D.; Tsai, J.-H.; Grätzel, C.; Wu, C.-G.; Zakeeruddin, S. M.; Grätzel, M. *ACS Nano* **2009**, *3*, 3103–3109.

(5) Mishra, A.; Fischer, M. K. R.; Bäuerle, P. *Angew. Chem., Int. Ed.* **2009**, *48*, 2474−2499 and references cited therein.

(6) (a) Lin, J. T.; Chen, P. C.; Yen, Y. S.; Hsu, Y. C.; Chou, H. H.; Yeh, M. C. P. *Org. Lett.* **2009**, *11*, 97–100. (b) Chen, K.-F.; Hsu, Y.-C.; Wu, Q.; Yeh, M.-C. P.; Sun, S.-S. *Org. Lett.* **2009**, *11*, 377–380. (c) Li, R.; Lv, X.; Shi, D.; Zhou, D.; Cheng, Y.; Zhang, G.; Wang, P. *J. Phys. Chem. C* **2009**, *113*, 7469–7479. (d) Zhang, G.; Bala, H.; Cheng, Y.; Shi, D.; Lv, X.; Yu, Q.; Wang, P. *Chem. Commun.* **2009**, 2198–2200. (e) Heredia, D.; Natera, J.; Gervaldo, M.; Otero, L.; Fungo, F.; Lin, C.-Y.; Wong, K.-T. *Org. Lett.* **2010**, *12*, 12–15. (f) Yang, H.-Y.; Yen, Y.-S.; Hsu, Y.-C.; Chou, H.-H.; Lin, J. T. *Org. Lett.* **2010**, *12*, 16–19.

(7) (a) Erten-Ela, S.; Yilmaz, M. D.; Icli, B.; Dede, Y.; Icli, S.; Akkaya, E. U. *Org. Lett.* **2008**, *10*, 3299–3302. (b) Fischer, M. K. R.; Wenger, S.; Wang, M.; Mishra, A.; Zakeeruddin, S. M.; Grätzel, M.; Bäuerle, P. *Chem. Mater.* **2010**, *22*, 1836–1845.

DOI: 10.1021/jo101831p Published on Web 10/25/2010

purification, and structural diversity, metal-free organic dyes are particularly attractive. While recent progress in power conversion efficiency (η) has reached a new record of η = 10.3% for organic dyes,[10] this still falls behind the performance of Ru dyes such as N719 (η = 11.18%)[3] and CYC-B11 (η = 11.5%)[4] and the challenging 15% efficiency. Strategies toward high-performance organic dyes include (i) increasing the light-harvesting efficiency, (ii) decreasing the tendency of dye aggregations, and (iii) reducing the chance of charge recombination of the injected electrons in the TiO_2 with the triiodide ions (I_3^-) in the electrolyte. It has recently been shown that cone-shaped organic dyes[7−9] derived from branched π-conjugated spacers are promising in the latter two issues.[8,9] One particular example is provided by truxene dyes (TDs),[9] which exhibited higher open-circuit voltages (V_{oc} = 0.69−0.75 V) and fill factors (ff = 0.70−0.74) than N719 for devices fabricated under the same condition. However, the relatively low short-circuit currents (J_{sc} = 6.86−7.89 mA/cm^2) preclude high η values (3.61−4.27%). In this context, isotruxene dyes (ITDs) are intriguing, because the ortho-para-substituted isotruxene core possesses a broader absorption profile toward visible light harvesting than the meta−meta substituted truxene isomer.[11,12] We report herein the synthesis and DSSC performance of four ITDs: **ITD**, **ITD-Hx**, **ITD-Th**, and **ITD-OM**. Our results show that the dye **ITD** retains the merits of high V_{oc} and ff values of the TDs and reaches a η value of 5.45%.

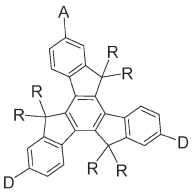

TDs

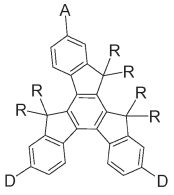

ITDs

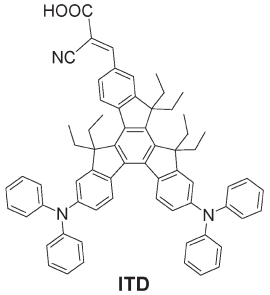

ITD

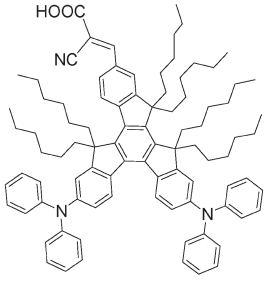

ITD-Hx

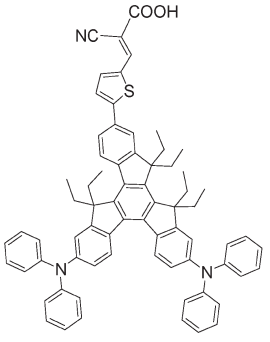

ITD-Th

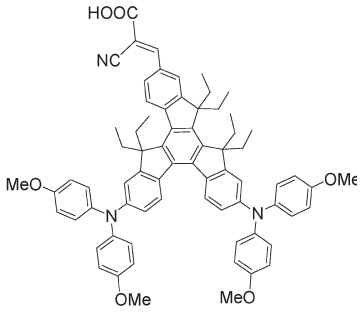

ITD-OM

Results and Discussion

Synthesis. We have recently developed facile synthetic methods toward construction of the unsymmetrical isotruxene scaffold.[13] Subsequent derivatizations of the parent isotruxene toward star-shaped π-conjugated systems have also been demonstrated.[12] However, selective substitution of the parent isotruxene with donor and acceptor groups as in ITDs is unknown and more likely to be very difficult. Thus, we have adopted one of our synthetic protocols for isotruxene to prepare prefunctionalized isotruxenes. Scheme 1 shows the synthesis of the isotruxene dibromides **6** and **7** from 3-pentanone and 4,4′-dibromobenzil through intermediates **1**−**5**. The facts of lower solubility and reagent compatibility caused by the bromo substituents force us to modify some of the reaction conditions. For example, the solubility of dibromoisotruxenone **5** is too low to be characterized with NMR spectroscopy. Consequently, the carbonyl reduction was achieved by directly reacting with boron trifluoride etherate (catalyst) and triethylsilane (hydride source) in the absence of solvents rather than by the Wulff−Kishner reaction.[14] In addition, to avoid metal−halide exchange, the previously used[12] base *n*-BuLi was replaced by *t*-BuOK for the alkylation of **6**. On the other hand, the presence of bromo substituents in the substrates is not always detrimental to the synthesis. For example, the intramolecular Friedel−Crafts acylation in **2** → **3** proceeds excellently with sulfuric acid. However, sulfuric acid led to water-soluble unknown compounds in the case of the bromo-free analogue, and a resolution of this problem by using polyphosphoric acid requires higher temperature (140 vs 70 °C) and longer reaction time (48 h vs 30 min).[13]

The alkylated isotruxene dibromides **7a** and **7b** are free of the solubility problem, and thus their subsequent derivatization is straightforward. Scheme 2 shows the synthesis of **ITD**, **ITD-Hx**, and **ITD-OM**. Formylation of **7a** and **7b** at the desired position was achieved by titanium tetrachloride and dichloromethyl methyl ether.[15] The palladium-catalyzed C−N coupling of the resulting **8a** or **8b** with diphenylamine or 4,4′-dimethoxyphenylamine afforded compounds **9a**, **9b**, and **9c**, which were finally converted to **ITD**, **ITD-Hx**, and **ITD-OM**, respectively, through the Knoevenagel condensation reaction with 2-cyanoacetic acid.

(8) (a) Thomas, K. R. J.; Hsu, Y.-C.; Lin, J. T.; Lee, K.-M.; Ho, K.-C.; Lai, C.-H.; Cheng, Y.-M.; Chou, P.-T. *Chem. Mater.* **2008**, *20*, 1830–1840. (b) Ning, Z.; Zhang, Q.; Wu, W.; Pei, H.; Liu, B.; Tian, H. *J. Org. Chem.* **2008**, *73*, 3791–3797. (c) Hagberg, D. P.; Yum, J.-H.; Lee, H.; De Angelis, F.; Marinado, T.; Karlsson, K. M.; Humphry-Baker, R.; Sun, L.; Hagfeldt, A.; Grätzel, M.; Nazeeruddin, M. K. *J. Am. Chem. Soc.* **2008**, *130*, 6259–6266. (d) Jiang, X.; Marinado, T.; Gabrielsson, E.; Hagberg, D. P.; Sun, L.; Hagfeldt, A. *J. Phys. Chem. C* **2010**, *114*, 2799–2805. (e) Chen, H.; Huang, H.; Huang, X.; Clifford, J. N.; Forneli, A.; Palomares, E.; Zheng, X.; Zheng, L.; Wang, X.; Shen, P.; Zhao, B.; Tan, S. *J. Phys. Chem. C* **2010**, *114*, 3280–3286.

(9) Ning, Z.; Zhang, Q.; Pei, H.; Luan, J.; Lu, C.; Cui, Y.; Tian, H. *J. Phys. Chem. C* **2009**, *113*, 10307–10313.

(10) Zeng, W.; Cao, Y.; Bai, Y.; Wang, Y.; Shi, Y.; Zhang, M.; Wang, F.; Pan, C.; Wang, P. *Chem. Mater.* **2010**, *22*, 1915–1925.

(11) Lang, K. F.; Zander, M.; Theiling, E. A. *Chem. Ber.* **1960**, *93*, 321–325.

(12) (a) Yang, J.-S.; Lee, Y.-R.; Yan, J.-L.; Lu, M.-C. *Org. Lett.* **2006**, *8*, 5813–5816. (b) Yang, J.-S.; Huang, H.-H.; Ho, J.-H. *J. Phys. Chem. B* **2008**, *112*, 8871–8878. (c) Yang, J.-S.; Huang, H.-H.; Liu, Y.-H.; Peng, S.-M. *Org. Lett.* **2009**, *11*, 4942–4945.

(13) Yang, J.-S.; Huang, H.-H.; Lin, S.-H. *J. Org. Chem.* **2009**, *74*, 3974–3977.

(14) Dailey, O. D., Jr. *J. Org. Chem.* **1987**, *52*, 1984–1989.

(15) Meltzer, P. C.; Bickford, P. H.; Lambert, G. J. *J. Org. Chem.* **1985**, *50*, 3121–3124.

SCHEME 1

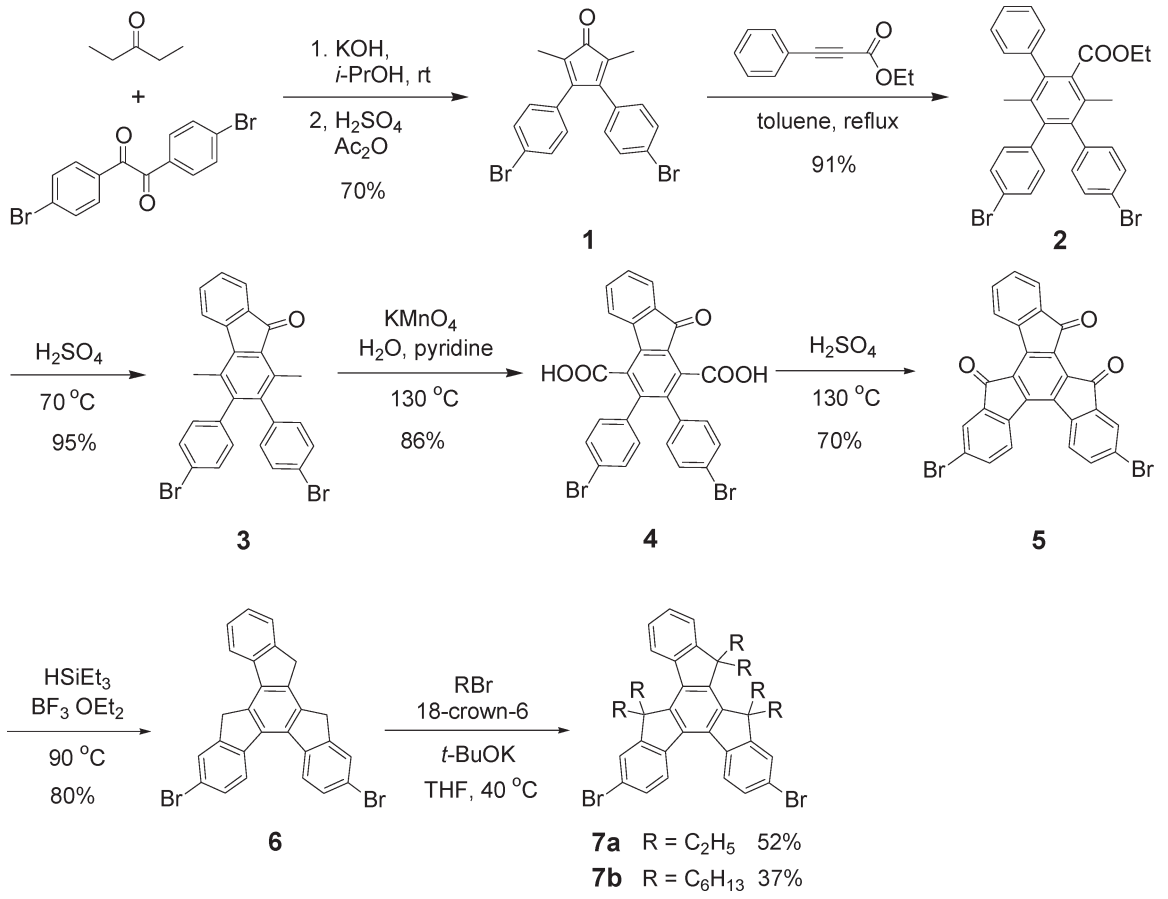

SCHEME 2

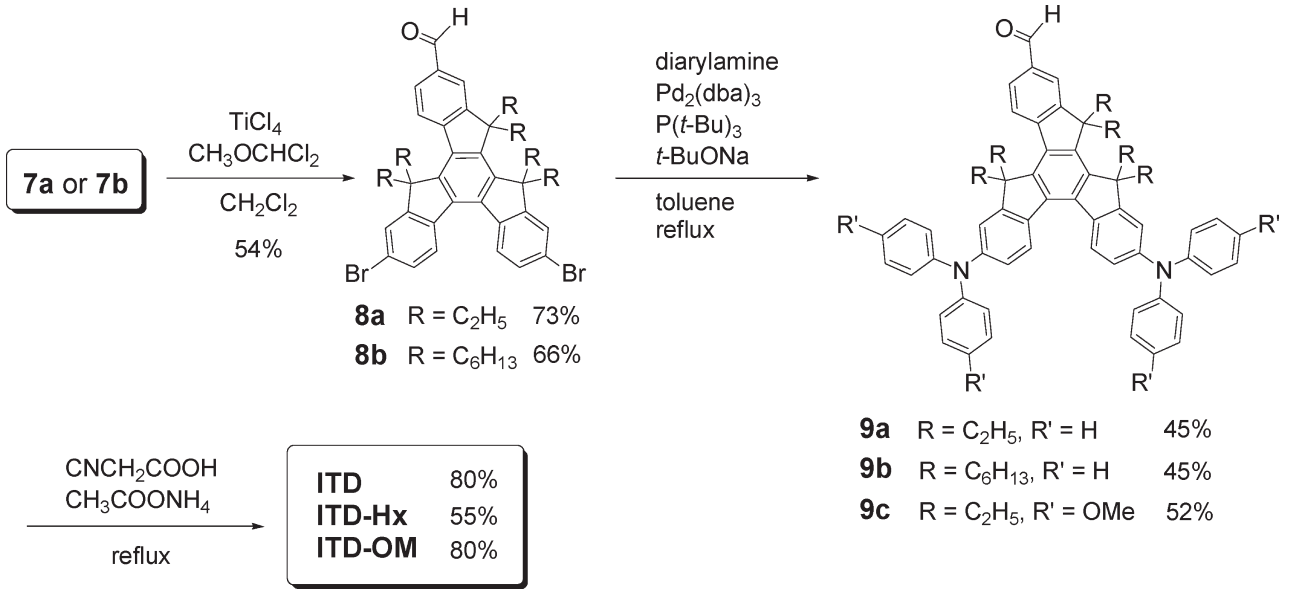

For **ITD-Th**, compound **7a** was iodinized to form **10** so that a thiophene group could be selectively introduced to the desired position via Suzuki−Miyaura coupling (Scheme 3). Subsequent amination of the resulting **11** removed the bromo substituents, and thus formylation of the intermediate **12** could proceed with the commonly used reagents *n*-BuLi and DMF. Again, the synthesis was accomplished by Knoevenagel reaction of the precursor **13** with 2-cyanoacetic acid.

Photophysical and Electrochemical Properties. The photophysical properties of the ITDs in THF are summarized in Table 1. The absorption profiles (Figure 1) display several vibration peaks in the region 250−400 nm and a broad

SCHEME 3. Synthesis of ITD-Th

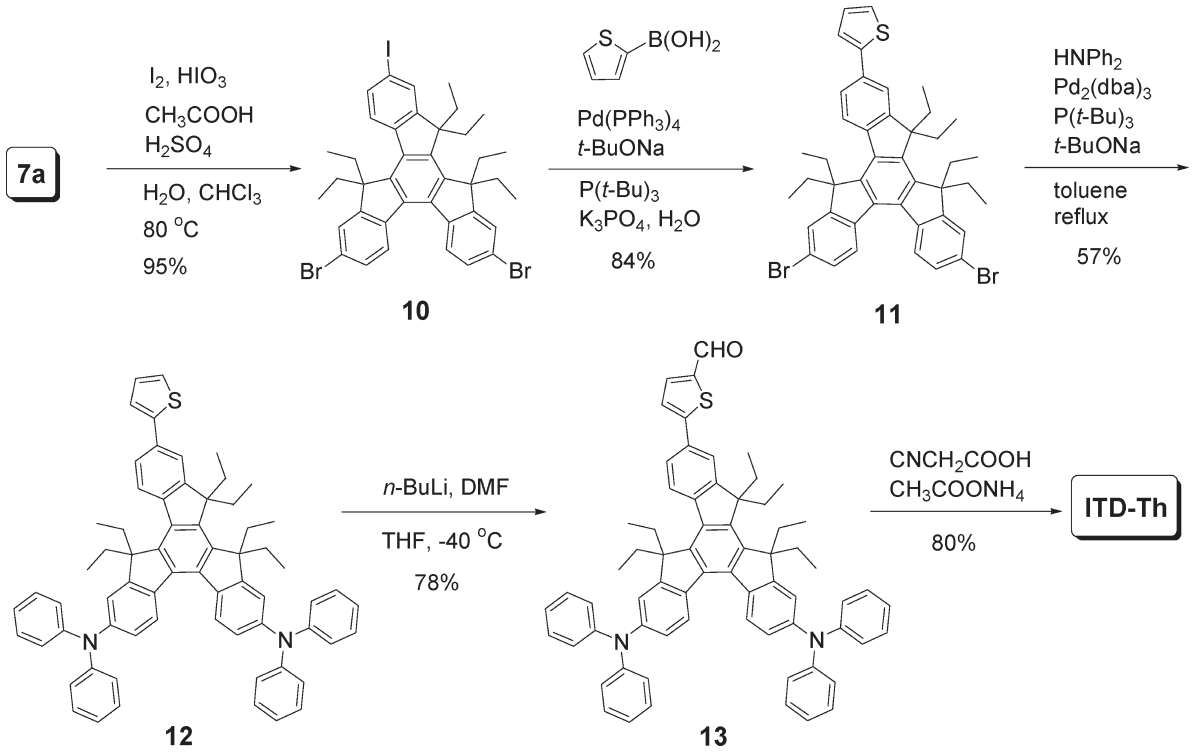

TABLE 1. Photophysical and Electrochemical Data for ITDs

dye	λ_{abs}[a] (nm)	log ε[b]	λ_{fl}[c] (nm)	Φ_{fl}[d]	E_{0-0}[e] (eV)	E_{ox}[f] (V)	E_{ox}*[g] (V)
ITD	383 (380)	4.71	529	0.28	2.37 (2.32)	0.88, 1.08	−1.49
ITD-Hx	383 (382)	4.71	525	0.27	2.35 (2.30)	0.88, 1.08	−1.47
ITD-Th	398 (395)	4.70	576	0.05	2.28 (2.23)	0.85, 1.06	−1.43
ITD-OM	388 (388)	4.72	577	0.29	2.32 (2.19)	0.68, 0.82	−1.64

[a]Maximum of the absorption band in THF. The maximum of the absorption band on 2 μm TiO_2 films is shown in parentheses. [b]Extinction coefficient of the absorption band in THF. [c]Maximum of the fluorescence spectra in THF. [d]Fluorescence quantum yield in THF. [e]Estimated from the onset of the absorption spectra in THF. Values in parentheses are from the onset of the spectra on the surface of TiO_2. [f]Oxidation potentials measured vs Fc^+/Fc in DCM were converted to normal hydrogen electrode (NHE) by addition of +0.63 V. [g]Energy of the LUMO of dyes estimated by $E_{ox} - E_{0-0}$.

shoulder with a maximum at ca. 480 nm. On the basis of our previous studies on isotruxene systems,[12] the former can be attributed to localized excitation and the latter to delocalized transition with a significant intramolecular charge-transfer character. More evidence for an intramolecular charge-transfer lowest singlet excited state for these ITDs include (a) structureless fluorescence spectra in THF (Figure 2), (b) the presence of vibrational structure in the delocalized absorption band for the donor-only intermeidate **12** but not for the donor−acceptor systems **13** and **ITD-Th** (Figure S1 in the Supporting Information), and (c) the distinct distribution of electron density in HOMO and LUMO, which are donor-localized and acceptor-localized, respectively (Figures 3). Compared to **ITD**, the additional thiophene and methoxy groups in **ITD-Th** and **ITD-OM**, respectively, result in a red shift of the absorption and fluorescence profiles (Figures 1 and 2) and a decrease of the 0−0 excitation energy (E_{0-0}) estimated from the absorption onset. In contrast, an elongation of the alkyl chains as in **ITD-Hx** is, as expected, of little influence in the molecular electronic

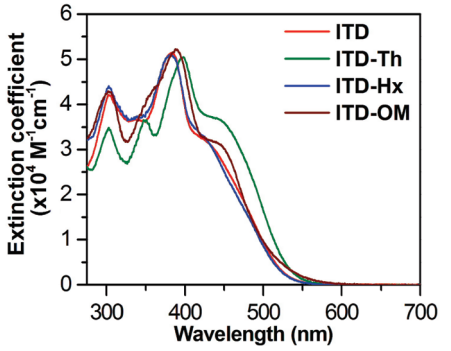

FIGURE 1. The absorption spectra of **ITD**, **ITD-Hx**, **ITD-Th**, and **ITD-OM** in THF.

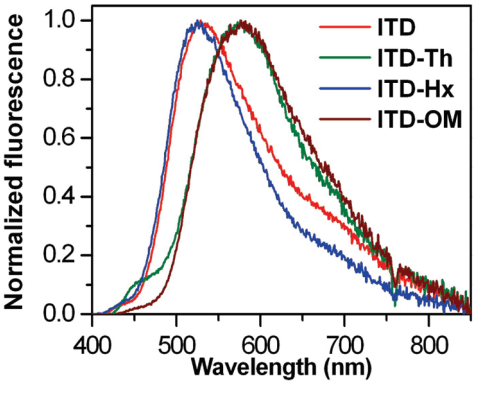

FIGURE 2. The fluorescence spectra of **ITD**, **ITD-Hx**, **ITD-Th**, and **ITD-OM** in THF.

properties. It should be noted that the 450-nm shoulder in the fluorescence profile of **ITD-Th** is due to contamination of a

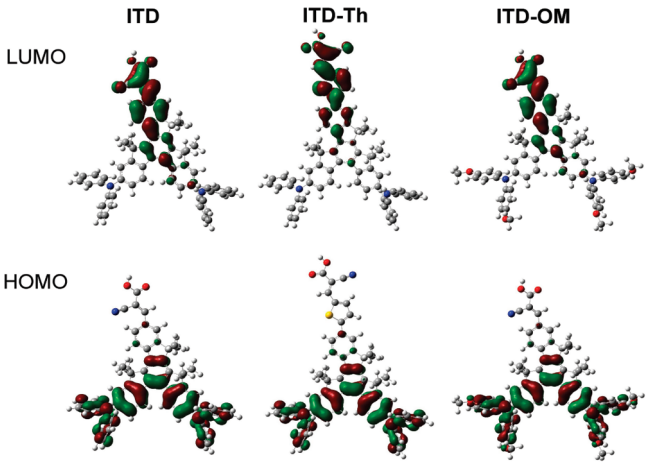

FIGURE 3. AM1-derived frontier molecular orbitals for **ITD**, **ITD-Th**, and **ITD-OM**.

trace amount of **12** (0.1%), which is strongly fluorescent (Figure S2 in the Supporting Information) with a fluorescence quantum yield (Φ_{fl}) of 0.79. The relatively lower Φ_{fl} value for **ITD-Th** as compared to the other ITDs might be attributed to thiophene-enhanced intersystem crossing toward the triplet excited states.[16]

Figure 4 compares the absorption spectra of the ITDs in dilute THF solutions and on the surface of TiO_2. The absorption maxima of the ITDs are nearly unchanged on going from dilute solutions to the thin solid films (Table 1). Regarding the absorption onset, it is red-shifted in a similar size (ΔE_{0-0} = 0.05 eV) for **ITD**, **ITD-Hx**, and **ITD-Th** but relatively larger for **ITD-OM** (ΔE_{0-0} = 0.13 eV). The small shift in the former compounds indicates that these unsymmetrical cone-shaped molecules are inapt to π-stacking and aggregations. A larger change in the absorption profile and thus a larger degree of intermolecular interactions for **ITD-OM** adsorbed on TiO_2 might be detrimental to its cell performance (vide infra).

The oxidation potentials (E_{ox}) of the ITDs were determined with cyclic voltammetry (CV) and differential pulse voltammetry (DPV) (Figure S3 in the Supporting Information), and the data with respect to normal hydrogen electrode (NHE) are shown in Table 1. Two reversible anodic curves are present for all four ITD dyes, which could be attributed to sequential oxidation of the two amino groups. This is in part based on the facts that oxidation of the parent isotruxene is much more difficult (E_{ox} = 1.42 V vs NHE) and that the E_{ox} value of π-extended isotruxene hydrocarbons is saturated at ca. 1.0 V (vs NHE).[12] The first oxidation potentials of **ITD**, **ITD-Hx**, and **ITD-Th** are similar (0.85−0.88 V), but it shifts negatively by ca. 200 mV for **ITD-OM**. In addition, the separation of the two oxidation peaks is smaller for **ITD-OM** (0.14 eV) than the other ITDs (0.20−0.21 eV). Both phenomena can be attributed to the electron-donating methoxy groups that raise the HOMO potential and reduce the Coulombic repulsion between the two charges. Nevertheless, the HOMO potentials of all four

(16) (a) Becher, R. S.; de Melo, J. S.; Maçanita, A. L.; Elisei, F. *J. Phys. Chem.* **1996**, *100*, 18683–18695. (b) Pina, J.; de Melo, J. S.; Burrows, H. D.; Galbrecht, F.; Nehls, B. S.; Farrell, T.; Scherf, U. *J. Phys. Chem. C* **2007**, *111*, 7185–7191.

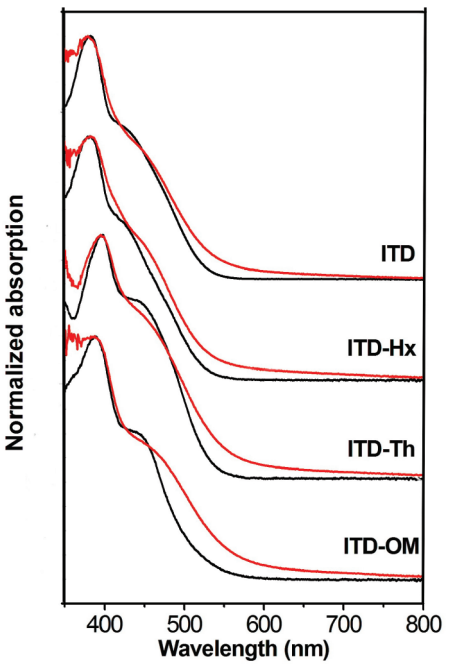

FIGURE 4. Comparison of the absorption spectra of **ITD**, **ITD-Hx**, **ITD-Th**, and **ITD-OM** in THF (black curve) and on 2 μm TiO_2 films (red curve).

TABLE 2. DSSCs Performance Parameters of Dyes[a]

dye	rel loading[b]	V_{OC} (V)	J_{SC} (mA/cm^2)	η (%)	ff	τ_R (ms)
ITD	1.00	0.75	10.13	5.45	0.72	0.73
ITD-Hx	0.73	0.76	7.31	3.64	0.66	0.72
ITD-Th	1.03	0.69	9.71	4.62	0.69	0.68
ITD-OM	0.96	0.67	5.53	2.48	0.67	0.58
N719	0.87	0.70	14.02	6.81	0.69	0.58

[a]Experiments were conducted with TiO_2 photoelectrodes with approximately 10 μm thickness and 0.16 cm^2 working area on the FTO (7 Ω/sq.) substrates. [b]The dye adsorption on TiO_2 relative to the dye **ITD**, which is 1.82×10^{-7} mol/cm^2.

ITDs (0.68−0.88 V) are more positive than that of the I^-/I_3^- redox couple (0.42 V vs NHE),[17] and thus regeneration of the oxidized dyes is thermodynamically feasible. The LUMO or excited-state oxidation potentials ($E_{ox}^* = E_{ox} - E_{0-0}$) of the ITDs ($E_{ox}^*$) are more negative than the conduction-band-edge energy level of the TiO_2 electrode (−0.5 V vs NHE),[17] which assures that the electron injection process is energetically favorable.

Photovoltaic Performance. Table 2 shows the performance statistics of DSSCs fabricated with the ITDs on nanocrystalline anatase TiO_2 particles and with liquid electrolyte of 0.05 M I_2, 0.1 M LiI, 0.5 M 1-methyl-3-propylimidazolium iodide, and 0.5 M *tert*-butylpyridine in acetonitrile. The cells have an effective area of 0.16 cm^2 and their performance was evaluated under AM 1.5 G illumination (100 mW cm^{-2}). The corresponding photocurrent−voltage ($J-V$) curves and the $J-V$ plot in the dark are shown in Figure 5, and the incident photocurrent conversion efficiencies (IPCE) are shown in Figure 6.

Among the four ITDs, the **ITD** cell exhibits the best power conversion efficiency (η = 5.45%), which reaches 80% of a N719-based DSSC fabricated and measured under similar

(17) Grätzel, M. *Nature* **2001**, *414*, 338–344.

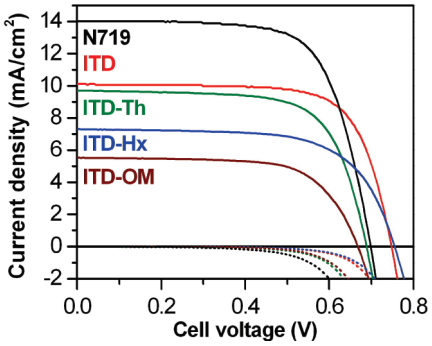

FIGURE 5. $J-V$ curves (solid curves) and dark current plots (dashed curves) of DSSCs based on the ITDs and N719 dyes.

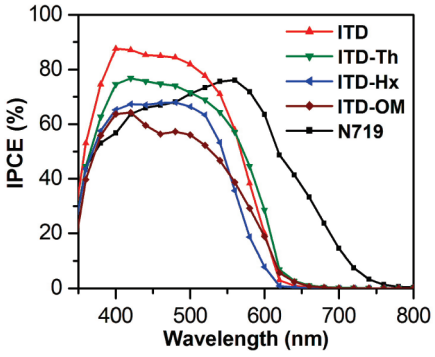

FIGURE 6. IPCE plots of DSSCs based on the ITDs and N719 dyes.

conditions (Table 2). Such a performance stems from high V_{oc} (0.75 V), ff (0.72), and IPCE (> 80% in the range 390−510 nm with a maximum of 88% at 400 nm) values. The observation of high V_{oc} for the DSSCs suggests that the processes of charge recombination between the injected electrons in TiO_2 and triiodide (I_3^-) in electrolyte are miminized.[18] This in turn indicates that the adsorbed dyes can effectively block the approach of electrolyte to the TiO_2 surface. While a high V_{oc} (0.76 V) is also displayed by the **ITD-Hx** cell, the cell is less efficient in ff and η, attributable to the lower J_{sc} value. In view of the parallel reduction (27−28%) in J_{sc} and the amount of dye adsorption on TiO_2 (Table 2) on going from **ITD** to **ITD-Hx**, the poorer cell performance for the latter can be attributed to less dye loading and thus less efficient light harvesting. In contrast, both the **ITD-Th** and **ITD-OM** cells have lower V_{oc} and enhanced dark current than the **ITD** cell, indicating that the $TiO_2 \rightarrow$ electrolyte charge recombination route becomes more significant. Further verification of this argument is provided by the measurement of transient photovoltage at open circuit (Figure 7). The resulting recombination lifetimes (τ_R) of the photoinjected electron with the redox couples for **ITD**, **ITD-Hx**, and **ITD-Th** are indeed higher than that for **ITD-OM** and N719 (Table 2). With a similar amount of dye loading for **ITD**, **ITD-Th**, and **ITD-OM**, it appears that an elongation of either the cone length (**ITD-Th**) or the cone radius (**ITD-OM**) would increase the chance of the electrolyte being

(18) (a) Hara, K.; Sato, T.; Katoh, R.; Furube, A.; Ohga, Y.; Shinpo, A.; Suga, S.; Sayama, K.; Sugihara, H.; Arakawa, H. *J. Phys. Chem. B* **2003**, *107*, 597–606. (b) Miyashita, M.; Sunahara, K.; Nishikawa, T.; Uemura, Y.; Koumura, N.; Hara, K.; Mori, A.; Abe, T.; Suzuki, E.; Mori, S. *J. Am. Chem. Soc.* **2008**, *130*, 17874–17881.

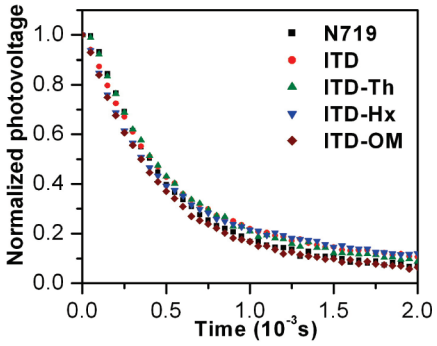

FIGURE 7. Transient photovoltage plots of DSSCs based on the ITDs and N719 dyes.

close to the TiO_2 surface. This might result from the presence of more void space near the surface of TiO_2 and/or larger pores between neighboring dye molecules, as schematically depicted in Figure 8. Other factors such as (a) a smaller driving force for regeneration of the oxidized dyes due to a higher HOMO potential and (b) a greater chance of self-quenching of the excited dyes due to dye aggregation (Figure 4) might also account for the relatively poor performance of the **ITD-OM** cell.

The relative cell performance of truxene- and isotruxene-based dyes might deserve a comment. For this purpose, the pair of **ITD-Th** and the truxene counterpart (**TD-Th**) are compared,[9] because they have the same donor, acceptor, and alkyl groups and differ only in the branched cores. To account for the difference in DSSC fabrication, the performance is better discussed relative to the corresponding reference cells of N719. The relative values of V_{oc}, J_{sc}, ff, and η are 95%, 66%, 111%, and 69% for **TD-Th** vs N719 and 99%, 69%, 100%, and 68% for **ITD-Th** vs N719. Both dyes have V_{oc} and ff comparable or superior to N719, but their J_{sc} are unsatisfactory. Overall, the η for **TD-Th** and **ITD-Th** is lower than that for N719. Although the light harvesting in the region of 550−600 nm for **ITD-Th** (ca. 40%) is more efficient than that for **TD-Th** (ca. 10%) in terms of the IPCE profiles, which might account for the slightly larger V_{oc} and J_{sc}, it is offset by the lower ff for **ITD-Th** vs **TD-Th** and thus results in a similar η value for both dyes.

Conclusions

We have synthesized a new class of cone-shaped organic sensitizers for DSSCs. The rigid, planar, and para-ortho-branched isotruxene spacer is critical for effective conjugation and light harvesting. The DSSC devices with the dye **ITD** have reached a power conversion efficiency of 5.45%, which is 80% of the Ru dye N719 fabricated under the same conditions. Further studies are required to understand the structure−property relationship in these unsymmetrical cone-shaped dyes in terms of the cone dimensions (length vs radius) and the relative positions of the donor and acceptor groups.

Experimental Section

General Methods. All the spectral and electrochemical data were collected at room temperature (23 ± 1 °C). The cyclic voltammetry (CV) and differential pulse voltammetry (DPV) were recorded on a CHI 612B electrochemical analyzer, and a

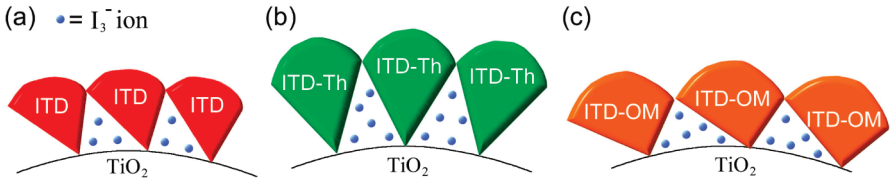

FIGURE 8. Schematic representation of the relationship of the molecular shape of (a) **ITD**, (b) **ITD-Th**, and (c) **ITD-OM** and the amount of electrolyte molecules near the surface of TiO_2.

glassy carbon served as the working electrode. The substrates are dissolved 1 mM in CH_2Cl_2 solution containing 0.1 M Bu_4NPF_6 as a supporting electrolyte. UV−visible spectra were measured on a Cary300 double beam spectrophotometer. Fluorescence spectra were recorded on an Edinburgh FLS920 spectrometer and corrected for the response of the detector. Fluorescence quantum yield was determined with an integrating sphere (150 mm diameter, $BaSO_4$ coating) for N_2-bubbled THF solution of the ITDs. The optical density of all solutions was about 0.1 at the wavelength of excitation, and an error of ±10% is estimated for the fluorescence quantum yields. The frontier molecular orbitals (FMOs) were derived by semiempirical (AM1)[19] level calculation. The optimized geometry results from a step-growth strategy: namely, structural optimization starts with the isotruxene segment and then optimized again for each time of adding one more segment like diphenylamine and thiophene until the full structure is reached. The ethyl or hexyl groups were replaced by methyl groups in order to expedite the calculations. The preparation of TiO_2 precursor and the electrode fabrication were carried out based on a previous report[20] with an autoclaved temperature of 240 °C. The film thickness measured by a profilometer (Dektak3, Veeco/Sloan Instruments Inc., USA) was about 10 μm. The TiO2 electrode with a 0.16 cm^2 geometric area was immersed in a acetonitrile/*tert*-butanol mixture (volume ratio 1:1) containing 3×10^{-4} M *cis*-di(thiocyanato)bis(2,2′-bipyridyl-4,4′-dicarboxylato)-ruthenium(II) bis(tetrabutylammonium) (N719, Solaronix S. A., Switzerland) or in EtOH solutions containing 3×10^{-4} M organic sensitizers for overnight. A platinized FTO was used as a counter electrode and was controlled to have an active area of 0.36 cm^2 by adhered polyester tape with a thickness of 60 μm. After rinsing with EtOH, the photoanode was placed on top of the counter electrode and tightly clipped together to form a cell. A 0.5 × 0.5 cm^2 cardboard mask was clipped onto the device to constrain the illumination area. The photoelectrochemical characterizations on the solar cells were carried out by using an Oriel Class A solar simulator (Oriel 91195A, Newport Corp.). Photocurrent−voltage characteristics of the DSSCs were recorded with a potentiostat/galvanostat (CHI650B, CH Instruments, Inc., USA) at a light intensity of 1.0 sun calibrated by an Oriel reference solar cell (Oriel 91150, Newport Corp.). The monochromatic quantum efficiency was recorded through a monochromator (Oriel 74100) at short circuit condition. The intensity of each wavelength was in the range of 1−3 mW/cm^2. The photovoltage transients of assembled devices were recorded with a digital oscilloscope (LeCroy, WaveSurfer 24Xs). Pulsed laser excitation was applied by a Q-switched Nd:YAG laser (Continuum, model Minilite II) with 1 Hz repetition rate at 532 nm and a 5 ns pulse width at half-height. The beam size was slightly larger than 0.5 × 0.5 cm^2 to cover the area of the device. The photovoltage of each device was adjusted by incident pulse energy to be 40 mV. The average electron lifetime can be estimated approximately by fitting a decay of the open circuit voltage transient with $\exp(-t/\tau_R)$, where t is time and τ_R is an average time constant before recombination.

(19) Dewar, M. J. S.; Zoebisch, E. G.; Healy, E. F.; Stewart, J. J. P. *J. Am. Chem. Soc.* **1985**, *107*, 3902–3909.
(20) Huang, C.-Y.; Hsu, Y.-C.; Chen, J.-G.; Suryanarayanan, V.; Lee, K.-M.; Ho, K.-C. *Sol. Energy Mater. Sol. Cells* **2006**, *90*, 2391–2397.

Materials. The synthesis of **1** was previously reported[21,22] and our melting points and ^{1}H NMR spectrum conform to the literature data.

Synthesis of 2. To a stirred solution of compound **1** (10.00 g, 24.0 mmol) and ethyl phenylpropiolate (4.36 g, 25.0 mmol) in toluene (15 mL) was heated to reflux for 24 h. The toluene was removed under reduced pressure, and the residue was recrystallized from MeOH to afford the white solid of **2** with a yield of 91%: mp 207−209 °C; ^{1}H NMR (400 MHz, $CDCl_3$) δ 0.93 (t, J = 7.2 Hz, 3H), 1.75 (s, 3H), 2.02 (s, 3H), 3.94 (q, J = 7.2 Hz, 2H), 6.78−6.48 (m, 4H), 7.27−7.40 (m, 9H); ^{13}C NMR (100 MHz, $CDCl_3$) δ 14.1, 18.4, 19.2, 61.3, 120 (×2), 127.5, 128.2, 129.6, 129.7, 131.2 (×2), 131.5, 131.7, 132.4, 135.1, 138.9, 139.0, 139.4, 139.5, 139.9, 141.6, 169.7; IR (KBr) 3053, 3024, 2978, 2933, 2872, 1722, 1592, 1493 cm^{-1}; EI-HRMS calcd for $C_{29}H_{24}Br_2O_2$ 562.0143, found 562.0133.

Synthesis of 3. The mixture of compound **2** (10.00 g, 17.7 mmol) and 17.7 M H_2SO_4 (100 mL) was heated at 70 °C for 30 min. After cooling to room temperature, the mixture was poured into H_2O. The precipitate was collected on a filter, washed with H_2O, and dried under vacuum to afford the yellow solid of **3** with a yield of 95%: mp 202−204 °C; ^{1}H NMR (400 MHz, $CDCl_3$) δ 2.27 (s, 3H), 2.35 (s, 3H), 6.76−6.82 (m, 4H), 7.28−7.34 (m, 5H), 7.49 (t, J = 7.6 Hz, 1H), 7.68−7.71 (m, 2H); ^{13}C NMR (100 MHz, $CDCl_3$) δ 15.6, 18.1, 120.7, 120.9, 123.6, 123.9, 128.4, 129.7, 130.5, 130.9, 131.0, 131.1, 131.5, 134.3, 135.0, 135.4, 138.0, 138.5, 142.3, 144.0, 146.7; IR (KBr) 3047, 2922, 2868, 1699, 1605 cm^{-1}; EI-HRMS calcd for $C_{27}H_{18}Br_2O$ 515.9724, found 515.9724.

Synthesis of 4. The mixture of compound **3** (5.00 g, 9.7 mmol) in pyridine (55 mL) and $KMnO_4$ (5.00 g, 31.6 mmol) in H_2O (2 mL) was heated at reflux for 2.5 h. Additional batches of 2 mL of H_2O and 5.00 g of $KMnO_4$ were added every 30 min for five times. The reaction mixture was further refluxed for 48 h. The hot solution (ca. 80 °C) was filtered to remove the MnO_2 solid and the solid was washed with MeOH. The filtrate was concentrated and the acid was recovered by addition of 1 M HCl. The precipitate was filtered and washed by H_2O and dried under vacuum to afford the yellow solid of **4** with a yield of 86%: mp > 300 °C; ^{1}H NMR (400 MHz, MeOH-d_4) δ 7.02 (d, J = 6.4 Hz 2H), 7.06 (d, J = 6.4 Hz, 2H), 7.35 (d, J = 8.0 Hz, 2H), 7.37 (d, J = 8.0 Hz, 2H), 7.45 (t, J = 7.6 Hz,1H), 7.59 (t, J = 7.6 Hz, 1H), 7.71 (d, J = 7.6 Hz, 1H), 7.74 (d, J = 7.6 Hz, 1H); ^{13}C NMR (100 MHz, MeOH-d_4) δ 123.0, 123.1, 123.6, 125.4, 130.0, 131.3, 131.9, 131.9, 132.9, 133.1, 133.2, 134.4, 135.2, 136.5, 136.7, 137.3, 139.3, 140.0, 142.8, 144.9, 169.6, 170.4, 191.6; IR (KBr) 3424, 2918, 2562, 1717, 1698, 1604, 1440, 1306, 1222 cm^{-1}; EI-HRMS calcd for $C_{27}H_{14}Br_2O_5$ 575.9208, found 575.9216.

Synthesis of 5. The mixture of powdered compound **4** (3.00 g, 5.2 mmol) and 17.7 M H_2SO_4 (90 mL) were added in a 250 mL round-bottomed flask and heated to 130 °C under stirring for 1 h. After cooling to room temperature, the solution was poured into ice. The precipitate was collected by filtration, washed with

(21) Goodson, F. E.; Novak, B. M. *Macromolecules* **1997**, *30*, 6047–6055.
(22) Mackay, D.; Pilger, C. W.; Wong, L. L. *J. Org. Chem.* **1973**, *38*, 2043–2049.

5% NaOH(aq) (3 × 30 mL) and then acetone, and dried under vacuum to afford the dark red solid of **5** with a yield of 70%. Due to its very poor solubility, the corresponding ^{1}H and ^{13}C NMR spectra were not determined: mp > 300 °C; IR (KBr) 3098, 3065, 1731, 1716, 1595, 1578 cm^{-1}; FAB-HRMS calcd for $C_{27}H_{10}Br_2O_3$ 539.8997, found 539.8997.

Synthesis of 6. The mixture of compound **5** (1.5 g, 2.77 mmol) in triethylsilane (50 mL) and boron trifluoride etherate (3 mL) was heated at reflux for 2 h. Additional batches of 3 mL of boron trifluoride etherate were added every 2 h for two times. The reaction mixture was further refluxed for 24 h. The precipitate was collected by filtration, washed with MeOH, and dried under vacuum to afford the white solid of **6** with a yield of 80%. Due to the very poor solubility of **6**, the corresponding ^{13}C NMR spectrum was not determined: mp 281−283 °C; ^{1}H NMR (400 MHz, $CDCl_3$) δ 3.95 (s, 1H), 4.20 (s, 1H), 7.36 (t, J = 7.2 Hz, 1H), 7.46 (t, J = 7.2 Hz, 1H), 7.56 (d, J = 7.2 Hz, 1H), 7.58 (d, J = 7.2 Hz, 1H), 7.61 (d, J = 7.2 Hz, 1H), 7.73 (s, 1H), 7.78 (s, 1H), 7.86 (d, J = 8.4 Hz, 1H), 8.26 (d, J = 8.4 Hz, 1H), 8.28 (d, J = 8.4 Hz, 1H); IR (KBr) 1457, 1414, 1367, 1083, cm^{-1}; FAB-HRMS calcd for $C_{27}H_{16}Br_2$ 497.9619, found 497.9618.

Synthesis of 7a. To a solution of compound **6** (2.00 g, 4.00 mmol) and potassium *tert*-butoxide (5 g, 45 mmol) in dry THF (80 mL) was added 18-crown-6 (cat. amount) at 0 °C. The solution was stirred for 30 min at room temperature, and then bromoethane (6.2 mL, 7.1 mmol) was added slowly. The solution was stirred further for another 120 min at 40 °C. The solution was cooled to 0 °C and an additional 6.2 mL of bromoethane was added. The solution was then stirred at 40 °C for 20 h. The solvent was removed and the residue was extracted with dichloromethane/water. The organic layer was dried with $MgSO_4$, filtered, and concentrated by rotary evaporation. The residue was purified by using column chromatography (silica gel, elution with hexane) to provide **7** with a yield of 52%: mp 208−210 °C; ^{1}H NMR (400 MHz, CD_2Cl_2) δ 0.09−0.31 (m, 18H), 2.04−2.19 (m, 6H), 2.58−2.70 (m, 4H), 2.92−3.00 (m, 2H), 7.35−7.38 (m, 3H), 7.46−7.50 (m, 3H), 7.60 (s, 1H), 8.21−8.28 (m, 3H); ^{13}C NMR (100 MHz, $CDCl_3$) δ 9.2, 9.2, 9.4, 29.7, 33.2, 33.4, 58.1, 58.5, 59.9, 120.6, 121.3, 123.0, 123.6, 124.0, 124.7, 125.3, 125.8, 126.5, 128.5, 128.6, 136.0, 136.2, 139.4, 139.4, 139.6, 139.7, 143.1, 144.5, 144.9, 150.8, 153.1, 154.1; IR (KBr) 2967, 2930, 2873, 1456 cm^{-1}; EI-HRMS calcd for $C_{39}H_{40}Br_2$ 666.1497, found 666.1484.

Synthesis of 7b. The procedure is similar to that of **7a** and an oil-like product was obtained with a yield of 37%; ^{1}H NMR (400 MHz, CD_2Cl_2) δ 0.48−1.11 (m, 66H), 1.98−2.10 (m, 6H), 2.46−2.54 (m, 4H), 2.87−2.90 (m, 2H), 7.29−7.36 (m, 3H), 7.44−7.50 (m, 3H), 7.60 (s, 1H), 8.21 (d, J = 8.4 Hz, 1H), 8.26 (d, J = 8.4 Hz, 2H); ^{13}C NMR (100 MHz, $CDCl_3$) δ 14.4, 14.4, 22.7, 23.0, 23.1, 24.2, 24.2, 24.4, 29.7, 29.8, 29.9, 31.6, 32.1, 32.1, 37.1, 40.9, 41.2, 56.9, 57.2, 58.6, 120.6, 121.0, 123.1, 123.7, 124.0, 124.5, 125.2, 125.6, 126.5, 128.4, 128.5, 135.6, 135.7, 138.9, 139.1, 139.2, 139.2, 143.9, 144.9, 145.3, 151.7, 154.0, 155.0; IR (KBr) 2955, 2926, 2856, 1466 cm^{-1}; FAB-HRMS calcd for $C_{63}H_{88}Br_2$ 1002.5253, found 1002.5214.

Synthesis of 8a. Under nitrogen atmosphere, **7a** (0.45 g, 0.67 mmol) was dissolved in dried CH_2Cl_2 (10 mL) at 0 °C. A batch of 1 M $TiCl_4$ in CH_2Cl_2 (8.3 mL) was added dropwise in 30 min with sufficient stirring. The purple reaction mixture was stirred for another 1 h at 0 °C, and then a solution of CH_3O-$CHCl_2$ (0.18 mL, 2.01 mmol) in 10 mL of CH_2Cl_2 was added dropwise over 10 min at 0 °C. The mixture was allowed to warm slowly and stirred for 1 h at room temperature. The purple mixture was poured into crushed ice. The organic layer was separated, and the aqueous layer was extracted with ethyl acetate. The combined organic fractions were washed with water and brine and finally dried over $MgSO_4$. The solution was concentrated under reduced pressure, and the residue was purified with column chromatography (silica gel, ethyl acetate/hexanes: 1/20) to provide **8a** with a yield of 73%: mp 113−115 °C; ^{1}H NMR (400 MHz, $CDCl_3$) δ 0.08−0.32 (m, 18H), 2.03−2.13 (m, 6H), 2.61−2.68 (m, 4H), 2.85−2.95 (m, 2H), 7.45−7.48 (m, 3H), 7.56 (s, 1H), 7.85 (s, 1H), 7.87 (d, J = 8.0 Hz, 1H), 8.20 (d, J = 8.0 Hz, 1H), 8.23 (d, J = 8.0 Hz, 1H), 8.23 (d, J = 8.0 Hz, 1H), 8.37 (d, J = 8.0 Hz, 1H), 10.08 (s, 1H); ^{13}C NMR (100 MHz, $CDCl_3$) δ 8.8, 8.9, 9.0, 29.7, 32.9, 32.9, 58.2, 58.5, 59.9, 121.2, 121.5, 121.5, 123.3, 124.0, 124.3, 125.0, 125.6, 129.0, 129.1, 129.3, 134.5, 136.7, 138.1, 139.2, 139.4, 144.9, 145.1, 146.3, 146.6, 152.0, 153.7, 154.2, 191.8; IR (KBr) 2965, 2931, 2873, 1962, 1603, 1461 cm^{-1}; FAB-HRMS calcd for $C_{40}H_{40}Br_2O$ 694.1446, found 694.1442.

Synthesis of 8b. The procedure is similar to that of **8a** with a yield of 66%: mp 52−54 °C; ^{1}H NMR (400 MHz, $CDCl_3$) δ 0.50−1.09 (m, 66H), 1.93−2.10 (m, 6H), 2.41−2.50 (m, 4H), 2.77−2.84 (m, 2H), 7.43−7.50 (m, 3H), 7.55 (s, 1H), 7.82 (s, 1H), 7.87 (d, J = 8.0 Hz, 1H), 8.18 (d, J = 8.0 Hz, 1H), 8.21 (d, J = 8.0 Hz, 1H), 8.38 (d, J = 8.0 Hz, 2H), 10.08 (s, 1H); ^{13}C NMR (100 MHz, $CDCl_3$) δ 14.3, 14.4, 14.4, 22.7, 23.0, 23.1, 24.2, 24.3, 24.4, 29.6, 29.7, 29.8, 31.6, 32.0, 32.1, 37.2, 40.8, 40.9, 57.1, 57.3, 58.7, 109.2, 120.9, 121.1, 121.2, 123.2, 124.0, 124.1, 124.6, 125.3, 128.6, 128.7, 128.9, 134.2, 136.0, 137.3, 173.4, 138.6, 138.8, 145.2, 145.4, 145.6, 146.7, 152.7, 154.2, 154.7, 191.4; IR (KBr) 2955, 2926, 2857, 1697, 1604, 1466, 1375 cm^{-1}; FAB-HRMS calcd for $C_{64}H_{88}Br_2O$ 1030.5205, found 1030.5189.

Synthesis of 9a. Compound **8a** (0.22 g, 0.3 mmol), diphenylamine (0.12 g, 0.7 mmol), $Pd_2(dba)_3$ (18 mg, 0.02 mmol), and sodium *tert*-butoxide (79.20 mg, 0.9 mmol) were mixed in a Schlenk tube. Under N_2, P(*t*-Bu)$_3$ (0.59 mL, 0.05 M in toluene, 0.03 mmol) and toulene (0.5 mL) were added. The mixture was heated to reflux with stirring for 24 h. The reaction mixture was then cooled to room temperature, diluted with H_2O, and extracted with ethyl acetate. The combined organic solution was washed with brine and dried over $MgSO_4$. The solution was concentrated under reduced pressure, and the residue was purified with column chromatography (silica gel, ethyl acetate/hexanes: 1/10) to provide **9a** with a yield of 45%: mp 112−114 °C; ^{1}H NMR (400 MHz, CD_2Cl_2) δ 0.24−0.38 (m, 18H), 1.90−1.94 (m, 3H), 2.00−2.07 (m, 3H), 2.11−2.17 (m, 3H), 2.56−2.60 (m, 3H), 2.63−2.68 (m, 3H), 2.82−2.88 (m, 3H), 6.96−7.29 (m, 24H), 7.83 (s, 1H), 7.83 (d, J = 8.4 Hz, 1H), 8.28 (d, J = 8.4 Hz, 1H), 8.31 (d, J = 8.4 Hz, 1H), 8.36 (d, J = 8.4 Hz, 1H), 10.05 (s, 1H); ^{13}C NMR (100 MHz, CD_2Cl_2) δ 9.2, 9.4, 30.2, 30.3, 30.6, 33.4, 33.5, 58.3, 58.8, 60.0, 117.6, 112.4, 122.0, 122.3, 122.4, 123.1, 123.1, 123.4, 124.2, 124.4, 124.5, 124.8, 129.3, 129.6, 134.9, 136.4, 145.6, 147.4, 147.8, 148.2, 152.6, 153.4, 153.6, 192.1; IR (KBr) 2965, 2929, 2873, 1964, 1594, 1492, 1484 1375, 1330, 1278 cm^{-1}; FAB-HRMS calcd for $C_{64}H_{60}N_2O_1$ 872. 4706, found 872.4705.

Synthesis of 9b. The procedure is similar to that of **9a** with a yield of 45%: mp 244−246 °C; ^{1}H NMR (400 MHz, CD_2Cl_2) δ 0.44−1.15 (m, 66H), 1.84−2.09 (m, 6H), 2.43−2.54 (m, 4H), 2.76−2.78 (m, 2H), 6.95−7.28 (m, 24H), 7.82 (s, 1H), 7.83 (d, J = 8.4 Hz, 1H), 8.28 (d, J = 8.4 Hz, 1H), 8.31 (d, J = 8.4 Hz, 1H), 8.38 (d, J = 8.4 Hz, 1H), 10.05 (s, 1H); ^{13}C NMR (100 MHz, CD_2Cl_2) δ 14.6, 14.8, 23.2, 23.5, 24.8, 24.9, 30.1, 30.3, 32.1, 32.6, 32.6, 37.6, 41.2, 41.4, 57.21, 57.5, 58.6, 117.5, 118.3, 121.6, 122.1, 122.7, 122.7, 123.1, 124.0, 124.0, 124.5, 128.7, 129.2, 134.4, 135.7, 136.6, 145.5, 146.0, 146.5, 146.8, 147.1, 147.8, 153.0, 154.0, 154.3, 191.6; IR (KBr) 2954, 2926, 2856, 1696, 1595, 1494, 1375, 1331, 1278 cm^{-1}; FAB-HRMS calcd for $C_{88}H_{108}N_2O$ 1208.8462, found 1208.8429.

Synthesis of 9c. The procedure is similar to that of **9a** with a yield of 52%: mp 136−138 °C; ^{1}H NMR (400 MHz, CD_2Cl_2) δ 0.22−0.35 (m, 18H), 1.85−1.91 (m, 3H), 1.97−2.02 (m, 3H), 2.09−2.14 (m, 3H), 2.51−2.56 (m, 3H), 2.61−2.66 (m, 3H), 2.79−2.84 (m, 3H), 6.84−7.10 (m, 20H), 7.81 (s, 1H), 7.82 (d, J = 8.0 Hz, 1H), 8.18 (d, J = 8.4 Hz, 1H), 8.21 (d, J = 8.4 Hz,

1H), 8.33 (d, J = 8.0 Hz, 1H), 10.04 (s, 1H); ^{13}C NMR (100 MHz, CD_2Cl_2) δ 9.2, 9.2, 9.4, 30.2, 30.3, 33.4, 33.5, 56.0, 58.2, 58.7, 59.8, 114.3, 115.0, 115.2, 119.2, 119.3, 122.0, 123.0, 123.9, 124.7, 126.6, 126.6, 129.3, 134.6, 134.7, 137.0, 137.3, 139.1, 141.5, 141.6, 145.1, 145.3, 147.6, 148.4, 148.7, 152.5, 153.2, 153.6, 156.1, 156.2, 192.2; IR (KBr) 2964, 2929, 2873, 1692, 1601, 1506, 1240 cm^{-1}; FAB-HRMS calcd for $C_{68}H_{69}N_2O_5$ 992.5128, found 992.5133.

Synthesis of 10. A mixture of compound **7a** (1.00 g, 1.5 mmol) and 14 mL of mixed solvents (CH_3COOH:H_2SO_4:H_2O:$CHCl_3$ = 100:5:20:8) was heated to 40 °C with stirring. The reagents HIO_3 (0.13 g, 0.8 mmol) and I_2 (0.38 g, 1.5 mmol) were then added. The solution was heated to 80 °C and stirred for 24 h. The solution was cooled to room temperature and extracted with CH_2Cl_2. The organic layer was washed with $Na_2S_2O_3$ and concentrated under reduced pressure, and the residue was purified with column chromatography (silica gel, hexanes) to provide **10** with a yield of 95%: mp 208−210 °C; ^{1}H NMR (400 MHz, $CDCl_3$) δ 0.23−0.30 (m, 18H), 1.97−2.13 (m, 6H), 2.54−2.63 (m, 4H), 2.80−2.85 (m, 2H), 7.42−7.46 (m, 3H), 7.53 (s, 1H), 7.62 (s, 1H), 7.65 (d, J = 8.4 Hz, 1H), 7.93 (d, J = 8.4 Hz, 1H), 8.16 (d, J = 8.4 Hz, 1H), 8.21 (d, J = 8.4 Hz, 1H); ^{13}C NMR (100 MHz, $CDCl_3$) δ 9.2, 9.3, 29.7, 33.2, 33.2, 58.1, 28.7, 59.9, 92.6, 120.8, 120.9, 123.1, 123.6, 124.7, 125.3, 125.6, 128.6, 128.8, 130.4, 134.8, 136.1, 136.7, 138.3, 139.2, 139.3, 143.4, 144.3, 144.5, 153.1, 153.4, 153.9; IR (KBr) 2965, 2928, 2871, 1457, 1366 cm^{-1}; FAB-HRMS calcd for $C_{39}H_{39}Br_2I$ 792.0463, found 792.0460.

Synthesis of 11. A mixture of compound **10** (0.30 g, 0.4 mmol), 2-thienylboronic acid (53 mg, 0.4 mmol), and $Pd(PPh_3)_4$ (44 mg, 0.04 mmol) was mixed in a Schlenk tube. Under N_2, P(t-Bu)$_3$ (0.63 mL, 0.05 M in toluene, 0.04 mmol), THF (2 mL), and K_3PO_4 (0.3 mL, 2 M in H_2O, 0.6 mmol) were added into the tube. The solution was stirred for 48 h at room temperature. The reaction mixture was diluted with H_2O and extracted with CH_2Cl_2. The combined organic solution was washed with brine, dried over $MgSO_4$, and concentrated under reduced pressure. The residue was washed with methanol and collected by filtration to provide **11** with a yield of 84%: mp > 300 °C; ^{1}H NMR (400 MHz, $CDCl_3$) δ 0.23−0.32 (m, 18H), 2.02−2.16 (m, 6H), 2.60−2.65 (m, 4H), 2.89−2.95 (m, 2H), 7.10 (t, J = 4.4 Hz, 1H), 7.30 (d, J = 6 Hz, 1H), 7.41 (d, J = 4.4 Hz, 1H), 7.2 (s, 1H), 7.44−7.46 (m, 3H), 7.52 (s, 1H), 7.55 (s 1H), 7.61(d, J = 8.0 Hz, 1H), 8.16−8.24 (m, 3H); ^{13}C NMR (100 MHz, $CDCl_3$) δ 8.9, 9.0, 9.0, 29.6, 33.0, 33.2, 58.0, 58.6, 59.8, 118.6, 120.9, 122.9, 123.3, 123.8, 124.1, 124.6, 124.9, 125.6, 128.0, 128.8, 129.0, 132.8, 136.4, 136.7, 139.2, 139.5, 139.7, 139.9, 143.5, 144.5, 144.9, 145.4, 152.1, 153.5, 154.5; IR (KBr) 1966, 2929, 2872, 1459, 1367, 809.8 cm^{-1}; FAB-HRMS calcd for $C_{43}H_{42}Br_2S$ 748.1374, found 748.1375.

Synthesis of 12. Compound **11** (0.40 g, 0.5 mmol), diphenylamine (0.19 g, 1.7 mmol), $Pd_2(dba)_3$ (50 mg, 0.05 mmol), and sodium *tert*-butoxide (184 mg, 1.9 mmol) were mixed in a Schlenk tube. Under N_2, P(t-Bu)$_3$ (1.33 mL, 0.05 M in toluene, 0.07 mmol) and toulene (1 mL) were added into the tube. The tube was heated to reflux with stirring for 24 h. The reaction mixture was then cooled to room temperature, diluted with H_2O, and extracted with ethyl acetate. The combined organic solution was washed with brine, dried over $MgSO_4$, and concentrated under reduced pressure. The residue was purified with column chromatography (silica gel, CH_2Cl_2/hexanes: 1/6) to provide **12** with a yield of 57%: mp 168−170 °C; ^{1}H NMR (400 MHz, CD_2Cl_2) δ 0.28−0.39 (m, 18H), 1.90−2.12 (m, 6H), 2.55−2.67 (m, 4H), 2.85−2.90 (m, 2H), 6.96−7.32 (m, 26H), 7.32 (d, J = 3.2 Hz, 1H), 7.55 (s, 1H), 7.62 (d, J = 9.6 Hz, 1H), 8.20 (d, J = 8.0 Hz, 1H), 8.27 (d, J = 8.0 Hz, 1H), 8.33 (d, J = 8.0 Hz, 1H); ^{13}C NMR (100 MHz, CD_2Cl_2) δ 9.3, 9.3, 9.4, 30.1, 33.4, 33.7, 58.1, 58.9, 59.9, 118.0, 118.6, 119.0, 122.5, 122.6, 123.0, 123.3, 123.3, 123.9, 124.4, 124.9, 125.1, 128.5, 129.6, 132.8, 136.7, 136.8, 137.1, 137.6, 138.5, 140.7, 144.2, 144.7, 145.1, 145.4, 147.2, 147.3, 148.3, 152.7, 153.1, 154.0; IR (KBr) 2966, 2930, 2873, 1593, 1492, 1280 cm^{-1}; FAB-HRMS calcd for $C_{67}H_{62}N_2S$ 926.4634, found 926.4636.

Synthesis of 13. To a solution of compound **12** (0.20 g, 0.2 mmol) in THF (15 mL) at −20 °C was added a solution of 1.6 M n-butyl lithium (0.15 mL, 0.2 mmol) over 20 min. Dry DMF (0.1 mL) was added at −40 °C with stirring for 10 min. The solution was warmed to room temperature over 10 min before being quenched (1 M NH_4Cl, 10 mL) and extracted with ethyl acetate. The combined organic solution was washed with brine, dried over $MgSO_4$, and then concentrated under reduced pressure. The residue was purified with column chromatography (silica gel, CH_2Cl_2/hexanes: 1/2) to provide **13** with a yield of 78%: mp 171−173 °C; ^{1}H NMR (400 MHz, CD_2Cl_2) δ 0.32−0.41 (m, 18H), 1.92−1.95 (m, 2H), 2.00−2.22 (m, 4H), 2.53−2.67 (m, 4H), 2.83−2.87 (m, 2H), 7.01−7.28 (m, 24H), 7.52 (d, J = 4 Hz, 1H), 7.63 (s, 1H), 7.69 (d, J = 8.0 Hz, 1H), 7.77 (d, J = 4 Hz, 1H), 8.26−8.33 (m, 3H), 9.87 (s, 1H); ^{13}C NMR (100 MHz, CD_2Cl_2) δ 9.5, 9.5, 9.6, 30.2, 33.5, 33.7, 58.1, 59.9, 109.6, 117.5, 118.2, 122.1, 122.7, 123.0, 123.9, 129.2, 137.6, 142.0, 145.0, 146.7, 152.7, 153.4, 182.2; IR (KBr) 2967, 2929, 2872, 1669, 1592, 1494, 1443, 1279 cm^{-1}; FAB-HRMS calcd for $C_{68}H_{62}N_2OS$ 954.4583, found 954.4597.

Synthesis of ITD. A mixture of **9a** (140 mg, 0.16 mmol), cyanoacetic acid (50 mg, 0.6 mmol), ammonium acetate (50 mg, 0.7 mmol), and acetic acid (5 mL) was heated at 130 °C for 5 h. After cooling to room temperature, it was precipitated by pouring into water. The resulting solid was filtered, washed thoroughly with water and methanol, and reprecipitated from dichloromethane by pouring into methanol to provide **ITD** with a yield of 80%. For DSSC fabrication, the compound was further purified by column chromatography (eluent EA/MeOH = 1/5): mp 282−284 °C; ^{1}H NMR (400 MHz, CD_2Cl_2) δ 0.26−0.38 (m, 18H), 1.90−1.96 (m, 2H), 2.01−2.14 (m, 4H), 2.54−2.63 (m, 2H), 2.64−2.68 (m, 2H), 2.82−2.85 (m, 2H), 6.96−7.29 (m, 24H), 7.98 (s, 1H), 8.04 (d, J = 8.8 Hz, 1H), 8.28 (d, J = 8.8 Hz, 1H), 8.31 (d, J = 8.8 Hz, 1H), 8.35 (d, J = 8.8 Hz, 1H), 8.36 (s, 1H); ^{13}C NMR (100 MHz, DMSO-d_6) δ 9.4, 9.4, 9.6, 29.6, 57.9, 58.6, 59.6, 117.3, 118.1, 122.6, 123.6, 123.7, 124.3, 124.4, 124.8, 124.9, 130.1, 135.4, 135.7, 136.9, 137.4, 138.5, 145.2, 145.3, 147.3, 147.7, 147.8, 152.2, 153.1, 153.6, 154.6, 164.0; IR (KBr) 3441, 2967, 2931, 2874, 1592, 1491, 1482, 1376, 1331, 1280 cm^{-1}; FAB-HRMS calcd for $C_{67}H_{61}N_3O_2$ 939.4764, found 939.4775

Synthesis of ITD-Hx. The procedure is similar to that of **ITD** with a yield of 55%: mp 256−258 °C; ^{1}H NMR (400 MHz, CD_2Cl_2) δ 0.64−1.10 (m, 66H), 1.83−2.13 (m, 6H), 2.45−2.55 (m, 4H), 2.79 (m, 2H), 6.94−7.27 (m, 24H), 8.01 (s, 1H), 8.08 (m, 1H), 8.27−8.34 (m, 3H), 8.50 (s, 1H); ^{13}C NMR (100 MHz, $CDCl_3$) δ 13.9, 14.0, 14.1, 22.4, 22.7, 24.0, 24.1, 29.4, 29.5, 29.7, 31.4, 31.8, 31.9, 31.9, 36.9, 40.6, 40.8, 56.6, 57.0, 58.0, 117.1, 118.1, 122.1, 122.6, 122.7, 123.3, 124.0, 124.0, 129.2, 129.8, 135.3, 135.6, 136.4, 136.8, 138.6, 145.6, 146.4, 147.0, 147.3, 147.8, 147.9, 153.3, 154.1, 154.4; IR (KBr) 3446, 2954, 2926, 2856, 1594, 1494, 1376, 1332, 1277 cm^{-1}; FAB-HRMS calcd for $C_{91}H_{109}N_3O_2$ 1275.8520, found 1275.8517.

Synthesis of ITD-OM. The procedure is similar to that of **ITD** with a yield of 80%: mp 276−278 °C; ^{1}H NMR (400 MHz, DMSO-d_6) δ 0.16−0.27 (m, 18H), 1.82−2.07 (m, 6H), 2.5 (m, 4H), 2.73−2.78 (m, 2H), 3.75 (s, 12H), 6.73 (d, J = 9.6 Hz, 1H), 6.75 (d, J = 9.6 Hz, 1H), 6.86 (s, 1H), 6.92 (d, J = 7.2 Hz, 8H), 6.96 (s, 1H), 7.05 (d, J = 7.2 Hz, 8H), 7.88 (d, J = 8.0 Hz, 1H), 7.95 (s, 1H), 8.00 (s, 1H), 8.10 (d, J = 8.4 Hz, 1H), 8.14 (d, J = 8.4 Hz, 1H), 8.18 (d, J = 8.4 Hz, 1H); ^{13}C NMR (200 MHz, DMSO-d_6) δ 8.5, 8.5, 8.7, 28.9, 32.1, 32.2, 55.2, 56.9, 57.6, 58.6, 112.7, 113.4, 114.9, 117.0, 118.2, 122.5, 123.4, 123.9, 124.1, 126.3, 129.2, 129.6, 132.8, 133.0, 136.1, 136.3, 137.9, 140.2,

140.3, 144.1, 144.2, 144.6, 147.8, 148.1, 151.5, 152.2, 152.8, 153.3, 155.6, 155.6, 163.5; IR (KBr) 3446, 2965, 2931, 2873, 2932, 1602, 1506, 1240 cm^{-1}; FAB-HRMS calcd for $C_{71}H_{69}N_3O_6$ 1059.5186, found 1059.5192.

Synthesis of ITD-Th. The procedure is similar to that of **ITD** with a yield of 80%: mp 234−236 °C; ^1H NMR (400 MHz, CD_2Cl_2) δ 0.29−0.40 (m, 18H), 1.91−2.17 (m, 6H), 2.56−2.70 (m, 4H), 2.83−2.88 (m, 2H), 6.97−7.30 (m, 24H), 7.59 (d, J = 4 Hz, 1H), 7.67 (s, 1H), 7.75 (d, J = 8.0 Hz, 1H), 7.87 (d, J = 4 Hz, 1H), 8.29 (d, J = 8.0 Hz, 2H), 8.33 (d, J = 8.0 Hz, 1H), 8.42 (s, 1H); ^{13}C NMR (100 MHz, CD_2Cl_2) δ 9.5, 9.5, 9.6, 30.2, 33.5, 33.7, 58.1, 59.0, 59.9, 115.9, 117.5, 118.1, 119.3, 122.1, 122.7, 123.0, 123.7, 124.0, 124.5, 124.9, 124.9, 129.2, 130.5, 134.4, 136.1, 136.8, 137.5, 138.0, 140.5, 142.8, 144.3, 144.6, 145.0, 146.9, 147.1, 147.8, 152.6, 152.7, 153.4, 156.3, 167.2; IR (KBr) 3445, 2966, 2930, 2872, 1717, 1586, 1482, 1278, cm^{-1}; FAB-HRMS calcd for $C_{71}H_{63}N_3O_2S$ 1021.4641, found 1021.4637.

Acknowledgment. We thank the National Science Council of Taiwan, ROC, for financial support.

Supporting Information Available: Absorption and fluorescence spectra of **12** and **13**, cyclic and differential pulse voltammograms for the ITDs, and ^1H and ^{13}C NMR spectra of new compounds. This material is available free of charge via the Internet at http://pubs.acs.org.